Impaired Autophagy in CD11b$^+$ Dendritic Cells Expands CD4$^+$ Regulatory T Cells And Limits Atherosclerosis in Mice

Marc Clement[1], Juliette Raffort[1,2], Fabien Lareyre[1,2], Dimitrios Tsiantoulas[1], Stephen Newland[1], Yuning Lu[1], Leanne Masters[1], James Harrison[1], Svetlana Saveljeva[3], Marcella KL Ma[4], Maria Ozsvar-Kozma[5], Brian Y H Lam[4], Giles SH Yeo[4], Christoph J Binder[5], Arthur Kaser[3], Ziad Mallat[1, 6]

[1]Division of Cardiovascular Medicine, University of Cambridge, Cambridge, UK; [2]Université Côte d'Azur, Institut National de la Santé et de la Recherche Médicale, Centre Mediterranéen de Recherche Moléculaire, University Hospital of Nice, France ; [3]Department of Gastroenterology and Hepatology, University of Cambridge; [4]MRC Metabolic Diseases Unit, University of Cambridge Metabolic Research Laboratories, Wellcome Trust-MRC Institute of Metabolic Science, Genomics and Transcriptomics Core, Addenbrooke's Hospital, Cambridge CB2 0QQ, UK; [5]Department of Laboratory Medicine, Medical University of Vienna and Center for Molecular Medicine (CeMM) of the Austrian Academy of Sciences, Vienna, Austria; [6]Institut National de la Santé et de la Recherche Médicale, Paris Cardiovascular Research Center, Paris, France.

***Running title*:** *Atg16l1*$^{-/-}$ DCs Expand Atheroprotective CD4$^+$ Tregs

Subject Terms:
Atherosclerosis
Vascular Disease

Address correspondence to:
Dr. Ziad Mallat
Division of Cardiovascular Medicine
University of Cambridge
Cambridge, UK
zm255@medschl.cam.ac.uk

DOI: 10.1161/CIRCRESAHA.119.315248

ABSTRACT

***Rationale*:** Atherosclerosis is a chronic inflammatory disease. Recent studies have shown that dysfunctional autophagy in endothelial cells, smooth muscle cells and macrophages, plays a detrimental role during atherogenesis, leading to the suggestion that autophagy-stimulating approaches may provide benefit.

***Objective*:** Dendritic cells (DCs) are at the crossroad of innate and adaptive immune responses and profoundly modulate the development of atherosclerosis. Intriguingly, the role of autophagy in DC function during atherosclerosis and how the autophagy process would impact disease development has not been addressed.

***Methods and Results*:** Here, we show that the autophagic flux in atherosclerosis-susceptible low-density lipoprotein receptor deficient (*Ldlr*$^{-/-}$) mice is substantially higher in splenic and aortic DCs compared to macrophages, and is further activated under hypercholesterolemic conditions. RNA sequencing and functional studies on selective cell populations reveal that disruption of autophagy through deletion of *Atg16l1* differentially affects the biology and functions of DC subsets in *Ldlr*$^{-/-}$ mice under high fat diet. *Atg16l1* deficient CD11b^{+} DCs develop a TGF-β-dependent tolerogenic phenotype and promote the expansion of regulatory T cells (Tregs), whereas no such effects are seen with *Atg16l1* deficient CD8α^{+} DCs. *Atg16l1* deletion in DCs (all CD11c-expressing cells) expands aortic Tregs *in vivo*, limits the accumulation of T helper cells type 1 (Th1), and reduces the development of atherosclerosis in *Ldlr*$^{-/-}$ mice. In contrast, no such effects are seen when *Atg16l1* is deleted selectively in conventional CD8α^{+} DCs and CD103^{+} DCs. Total T cell or selective Treg cell depletion abrogates the atheroprotective effect of *Atg16l1* deficient DCs.

***Conclusions*:** In contrast to its pro-atherogenic role in macrophages, autophagy disruption in DCs induces a counter-regulatory response that maintains immune homeostasis in *Ldlr*$^{-/-}$ mice under high fat diet and limits atherogenesis. Selective modulation of autophagy in DCs could constitute an interesting therapeutic target in atherosclerosis.

Keywords:
Atherosclerosis; autophagy; immune system.

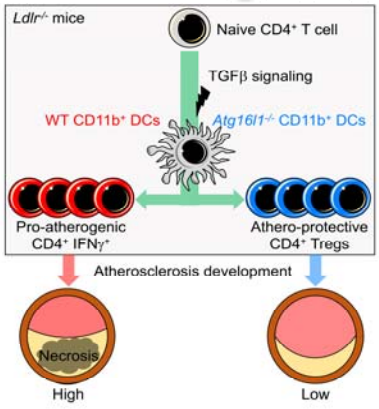

Non-standard Abbreviations and Acronyms:

A20 – (TNFAIP3: Tumor necrosis factor, alpha-induced protein 3)
Aire – Autoimmune regulator
Akt – (PKB: Protein kinase B)
αSMA – alpha smooth muscle actin
Atg – Autophagy-related protein
Atg16l1 cKO – Autophagy-related protein 16l1 conditional knock out
BATF3 – Basic Leucine Zipper ATF-Like Transcription Factor 3
CANTOS – Canakinumab Antiinflammatory Thrombosis Outcome Study
cDCs – conventional dendritic cells
Clec9a – C-Type Lectin Domain Containing 9A
CQ – Chloroquine
CTLA-4 – cytotoxic T-lymphocyte-associated protein 4
FACS – Fluorescence-activated cell sorting
FLT3 – fms-related tyrosine kinase 3
Foxj1 – Forkhead box protein J1
Foxp3 – Forkhead box P3
GFP – Green fluorescent protein
Havcr1 (Tim1) – Hepatitis A virus cellular receptor 1 (T-cell immunoglobulin and mucin domain 1)
HDL – High density lipoprotein
HFD – High fat diet
IFN-γ – Interferon gamma
IRF – Interferon regulatory factor
LC3 – Microtubule-associated protein 1A/1B-light chain 3
Ldlr – Low density lipoprotein receptor
MHC – Major histocompatibility complex
mir – micro ribonucleic acid
MOMA – Monocyte/Macrophage
mTOR – mammalian target of rapamycin
NLRP3 – NOD-like receptor family, pyrin domain containing 3
NOD – nucleotide-binding oligomerization domain
OVA – Ovalbumin
oxLDL – oxidized low density lipoprotein
pDCs – plasmacytoid dendritic cells
PI3K – Phosphoinositide 3-kinase
RBJP – Recombination Signal Binding Protein For Immunoglobulin Kappa J
RNA-seq – Ribonucleic acid sequencing
Slc15a2 – Solute carrier 15a2
SMC – smooth muscle cell

Sphk1 – Sphingosine kinase 1
TCF4 – Transcription factor 4
Tfh – T follicular helper
TGF-β – The transforming growth factor beta
Th1 – T helper 1
Treg – T regulatory
Vdr – Vitamin D receptor
WT – Wild type
YFP – Yellow fluorescent protein
Zbtb46 – Zinc Finger And BTB Domain Containing 46

INTRODUCTION

Extensive basic, pre-clinical and translational studies have validated the inflammatory hypothesis of atherosclerosis [1]. This concept has recently been nicely supported by the results of the CANTOS trial, which showed a significant reduction of cardiovascular events in patients with stable coronary artery disease and residual inflammation after treatment with canakinumab, a monoclonal anti-IL-1β antibody [2]. However, the relatively limited size effect of canakinumab and the failure of other anti-inflammatory therapies to alter the disease process in humans [3] crucially highlight the importance of a better understanding of the complex regulation of the immune system in the context of atherosclerosis.

Autophagy has recently emerged as a major modulator of a variety of cellular functions with high relevance to the development and progression of atherosclerosis [4]. Dysfunctional autophagy in atherosclerosis promotes apoptosis and senescence of endothelial cells [5], premature senescence of vascular smooth muscle cells (SMCs) [6], disturbs the cholesterol efflux pathway [7] and activates NLRP3 inflammasome in macrophages [8], and impairs the efferocytosis of apoptotic cells [9], all processes involved in plaque inflammation, progression and complications.

The relevance of autophagy in cells of the adaptive immune system to the development of atherosclerosis has received little attention. A recent study reported decreased atherosclerosis in mice with *Atg7* deletion in T cells [10]. The atheroprotective effect could not be attributed to a reduction of T cell mediated inflammation, because *Atg7* deficient T cells produced higher levels of the pro-atherogenic IFN-γ. However, *Atg7* deficiency in T cells was associated with an unexplained reduction of plasma cholesterol levels, which may have accounted for the atheroprotective effects. Given that dysfunctional autophagy may impair T helper cell differentiation, effector cell activation [11] and anergy [12], memory formation [13], as well as regulatory T cell (Treg) responses [14], addressing the role of autophagy in selective T cell subsets is necessary for a better understanding of the relevance of those processes to atherogenesis.

Dendritic cells (DCs) are professional antigen-presenting cells at the crossroad of innate and adaptive immune responses. DCs originate from a dendritic cell progenitor in the bone marrow. Transcription factors influencing DC subset development include zinc finger and BTB domain containing 46 (Zbtb46) for pre-classical DCs, which also require BATF3 and IRF8 to differentiate into $CD103^+$ ($CD8\alpha^+$ in lymphoid tissue) cDCs, or RBJP and IRF4 to give rise to $CD11b^+$ cDCs. In contrast, E2-2 (TCF4) is required for differentiation of the DC progenitor into plasmacytoid DCs. DC subsets may promote or limit atherogenesis through modulation of both innate and adaptive immune responses [15, 16].

Although it is dispensable for DC development, autophagy is involved in several biological processes relevant to DC functions, including DC maturation, responses to toll-like receptor stimulation and cytokine production, migration, antigen presentation and cross-presentation, and T cell activation (reviewed in [17]). DCs profoundly alter the development of atherosclerosis through effects on lipid metabolism, T cell priming, activation and differentiation, and modulation of Treg responses [15, 18-20]. Intriguingly, however, no study has addressed the role of autophagy in modulating DC functions during the development of atherosclerosis. Here, we aimed to fill this gap of knowledge and examined the impact of dysfunctional autophagy in distinct DC subsets on the immune responses during atherosclerosis. To modulate autophagy in DCs, we have deleted ATG16L1, which binds ATG5 and links the isolation membrane to the formation of the autophagosome [21, 22].

METHODS

Detailed methods are described in the online supplement.

All the experiments were approved by the local ethics committee and were performed under Home Office, UK license PA4BDF775. All the mice were on a C57Bl/6J genetic background. Female *Ldlr*$^{-/-}$ mice (6-8 week-old) were lethally irradiated (9.5 Gy), then injected i.v. (tail vein) with 1x10^7 bone marrow cells from donor mice. After 4 weeks of recovery, mice were fed a chow or high fat diet (21 % Fat, 0.15 % Cholesterol, Special Diet Services) for 8 weeks. Female littermate *CD11c*$^{Cre-}$ *Atg16l1*$^{flox/flox}$ and *CD11c*$^{Cre+}$ *Atg16l1*$^{flox/flox}$, as well as female littermate *Clec9a*$^{Cre-}$ *Atg16l*$^{flox/flox}$ and *Clec9a*$^{Cre+}$ *Atg16l1*$^{flox/flox}$, were used as bone marrow donors to reconstitute lethally irradiated *Ldlr*$^{-/-}$ animals.

RESULTS

HFD induces autophagy in aortic CD103$^+$ and splenic CD11b$^+$ DCs in Ldlr$^{-/-}$ mice.

Using bone marrow transfer from LC3-GFP mice [23] to *Ldlr*$^{-/-}$ mice, we first studied the modification of the autophagic-flux in dendritic cells after long term HFD feeding. In the spleen, DCs and more particularly cDCs, express high levels of LC3-GFP (Figure 1A) compared to monocytes, B cells or T cells (Online Figure I A-B), and this may be further enhanced by the HFD in CD11b$^+$ DCs (Figure 1B-C). In the aorta, CD103$^+$ DCs express the highest levels of LC3-GFP, followed by CD11b$^+$ DCs, CD11b$^-$CD103$^-$ DCs and macrophages (Figure 1D & Online Figure I C). HFD feeding did not change LC3-GFP expression in aortic DCs and macrophages (Online Figure I C). We confirmed by immunostaining that CD11c$^+$MHCII$^+$LC3$^+$ cells were found in the atherosclerotic plaque (Figure 1E). In order to know if the autophagic flux was active in DCs after HFD feeding, we used chloroquine (CQ) injection in vivo to inhibit autophagosome fusion with lysosomes and limit the degradation of LC3-GFP. LC3-GFP expression in splenic CD11b$^+$ DCs increased in the presence of CQ, suggesting that this was an active process (Figure 1F). However, CQ did not affect LC3-GFP expression in splenic CD8α^+ DCs. In the aorta, CQ significantly enhanced the expression of LC3-GFP in CD103$^+$ DCs, whilst no changes were observed in the other subsets (Figure 1G). Although a short-term injection of CQ can only inform about the activity of the autophagic flux at a specific time point (during the 2 days between CQ injection and mouse sacrifice), the data indicate that the autophagic flux is active both in splenic and aortic DCs under HFD.

Atg16l1 deficiency in CD11c expressing cells alters splenic T cell expansion and promotes CD4$^+$ Tregs in Ldlr$^{-/-}$ mice after HFD.

To examine whether autophagy in DCs plays a role in atherosclerosis, bone marrow from *Atg16l1$^{flox/flox}$ Cd11c^{Cre+}* (designated thereafter as *Atg16l1* cKO) or *Cd11c^{Cre-}* (designated thereafter as controls) littermate mice was transferred into *Ldlr$^{-/-}$* recipient mice. After 4 weeks of recovery, mice were fed a HFD for 8 weeks. At sacrifice, plasma total cholesterol, HDL-cholesterol, triglycerides, and weight were not different between the two groups (Online Figure II). Phenotyping of the spleen by flow cytometry revealed a significant reduction of spleen cellularity in *Atg16l1* cKO as compared to control *Ldlr$^{-/-}$* mice (Figure 2A). No differences in the numbers of DC subsets were observed between the two groups (Figure 2B-C). However, DCs of *Atg16l1* cKO *Ldlr$^{-/-}$* mice showed a reduction in MHCII expression (Figure 2D) without differences in CD80 (Figure 2E), as compared to DC from control *Ldlr$^{-/-}$* mice. Interestingly, deletion of *Atg16l1* in DCs was associated with a reduction of the numbers of splenic CD8$^+$ and CD4$^+$ T cells (Figure 2F), without affecting their expression of CD44 (memory T cells) (Figure 2G). In parallel, we found that the proportion of CD4$^+$ regulatory T cells was increased in *Atg16l1* cKO compared to control *Ldlr$^{-/-}$* mice (Figure 2H). B cells, germinal center (GC) B cells and T follicular helper (Tfh) cells, as well as immunoglobulin production (total and oxidized lipoprotein-specific), were not statistically different between the two groups (Online Figure III). Other splenic myeloid populations, including neutrophils and monocytes/macrophages, were likewise similar ($p>0.05$) between the two groups (Online Figure IV). Importantly, we confirmed that the DC and T cell phenotype described above was not observed under normo-cholesterolemic conditions (Online Figure V), suggesting a role for DC expression of *Atg16l1* in shaping the response of the immune system to HFD-induced atherosclerosis.

Atg16l1 deficiency in DCs promotes accumulation of CD4$^+$ Tregs in the aortas of HFD fed Ldlr$^{-/-}$ mice and limits the development of atherosclerosis.

Analysis of immune cell composition of aortas from *Atg16l1* cKO and control *Ldlr$^{-/-}$* mice showed no differences in the accumulation of DC subsets (Figure 3A), macrophages (Online Figure VI A), or T cells (Online Figure VI B). However, *Atg16l1* cKO *Ldlr$^{-/-}$* mice showed a significant reduction in the proportion of aortic CD4$^+$ IFNγ^+ cells, within the CD45$^+$ cell population, as compared to control *Ldlr$^{-/-}$* mice (Figure 3B). No differences in aortic CD8$^+$ IFNγ^+ cells were observed between the 2 groups (Online Figure VI C). In parallel, we found an enrichment in CD4$^+$ Tregs within aortic CD45$^+$ cells of *Atg16l1* cKO compared to control *Ldlr$^{-/-}$* mice (Figure 3C). The predominant accumulation of CD4$^+$ Tregs over Th1 cells in the aortas of *Atg16l1* cKO *Ldlr$^{-/-}$* mice was associated with a significant reduction of atherosclerosis development at the level of the aortic root (Figure 3D) and in the "en face" thoracic aorta (Figure 3E). On aortic cross sections, we found no statistically significant differences in percentages of MOMA-2$^+$ foam cells (Online Figure VI D), infiltrated CD3$^+$ cells (Online Figure VI E) and αSMA$^+$ SMCs (Online Figure VI F) between the two groups of mice. However, acellular 'necrotic' core area within the lesions was significantly smaller in *Atg16l1* cKO compared to control *Ldlr$^{-/-}$* mice (Figure 3F).

T cell depletion abolishes the atheroprotective effect associated with ATG16L1 deficient dendritic cells.

The major changes in the immune response associated with atheroprotection occurred in T cells. Because, a reduction in Th1 and an increase in Treg responses may confer a strong atheroprotective effect [24, 25], we investigated the requirement for T cells in mediating atheroprotection in *Atg16l1* cKO mice. We repeated the experiment in the presence of T cell depleting antibodies (anti-CD4/anti-CD8). No statistical difference was found in the extent of splenic T cell depletion achieved in *Atg16l1* cKO and control *Ldlr$^{-/-}$* mice (Figure 4A). Treatment with anti-CD4/anti-CD8 antibodies also led to CD8α^+, but not CD11b$^+$, DC depletion in spleen (data not shown). T cell depletion abolished the atheroprotection associated with autophagy deficient DCs in the thoracic aorta (Figure 4B), and even led to a bigger lesion size at the level

of the aortic root in *Atg16l1* cKO compared to control *Ldlr*$^{-/-}$ mice (Figure 4C). Lesions of T cell-depleted *Atg16l1* cKO *Ldlr*$^{-/-}$ mice contained significantly less foam cells (Figure 4D), similar ($p>0.05$) amount of αSMA^+ SMCs (Figure 4E), but significantly bigger acellular "necrotic" core (Figure 4F) compared to lesions of control *Ldlr*$^{-/-}$ mice, consistent with their bigger size and advanced stage of development.

Atg16l1 deficiency in CD8α$^+$ (and related CD103$^+$) DCs does not impact CD4$^+$ Tregs and does not protect from atherosclerosis.

To gain further insights into the DC subset responsible for the atheroprotective effect, we used *Clec9a*$^{Cre+}$ mice to target committed DC precursors and their progeny (conventional DCs but not pDCs nor monocyte-derived DCs [26]. We first examined the efficiency of *Atg16l1* deletion in FACS purified splenic CD8α$^+$ DCs and CD11b$^+$ DCs. We found that while *Cd11c*$^{Cre+}$ completely abrogated the expression of *Atg16l1* in both CD8α$^+$ and CD11b$^+$ DCs, *Clec9a*$^{Cre+}$ was efficient only in CD8α$^+$ DCs (~80% reduction of *Atg16l1* expression) **(**Figure 5A). This is consistent with the high expression of Clec9a on splenic CD8α$^+$ DCs. Splenic CD11b$^+$ cDCs do not express Clec9a but a previous study showed that they derive from a Clec9a-expressing committed DC precursor [26]. Our finding that *Atg16l1* expression was only partially reduced (~50%, $p=0.08$, control CD11b$^+$ DC vs *Clec9a*$^{cre+}$ *Atg16l1*^{flox} CD11b$^+$ DC) in splenic CD11b$^+$ DCs is consistent with the fact that only 50% of splenic CD11b$^+$ DCs showed YFP labeling in *Clec9a*$^{Cre+}$ *Rosa*$^{+/EYFP}$ mice, due to incomplete penetrance of Cre-mediated recombination in DC precursors [26]. Thus, *Clec9a*$^{Cre+}$ mice allow to efficiently manipulate gene expression only in CD8α$^+$ (and related CD103$^+$) cDCs. Bone marrow transfer experiments into irradiated *Ldlr*$^{-/-}$ mice using *Atg16l1*$^{flox/flox}$ *Clec9a*$^{Cre+}$ or control bone marrow cells revealed no differences in the proportions of splenic DC subsets (Figure 5B) and CD4$^+$ and CD8$^+$ T cells (Figure 5C), nor in the percentages of CD4$^+$ Tregs and Th1 cells (Figure 5D-E) after 8 weeks of HFD. This phenotype was not associated with any difference in atherosclerosis development (Figure 5F-G). Aortic accumulation of immune cells analyzed by flow cytometry (Online Figure VII), and plaque composition studied using immuno-fluorescent microscopy (foam cells, T cells, SMCs and acellular area) were similar ($p>0.05$) between the two groups (Online Figure VIII). Finally, lipid profiles and weight gain did not differ between the two groups (Online Figure IX). Thus, the atheroprotective phenotype associated with autophagy deficiency in CD11c$^+$ is not due to autophagy deficiency in CLEC9a$^+$ progenitor derived cDCs (including CD8α$^+$ cDCs), but is likely to be explained by a deficiency of autophagy in conventional and monocyte-derived CD11b$^+$ DCs.

Atg16l1 deficiency differentially alters gene expression in CD8α$^+$ and CD11b$^+$ DCs in Ldlr$^{-/-}$ mice fed a high fat diet.

To further understand how *Atg16l1* deficiency in CD11b$^+$ but not CD8α$^+$ DCs favors the expansion of CD4$^+$ Tregs upon HFD feeding in *Ldlr*$^{-/-}$ mice and prevents atherosclerosis, we purified splenic DCs (after bone marrow transplantation and 8 weeks of HFD) and analyzed their transcriptomic signature by RNA-seq (Figure 6A & Online Table I). We found that *Atg16l1* deficient CD8α$^+$ and CD11b$^+$ DCs differentially expressed 215 and 165 genes, respectively, as compared with their respective WT control DCs (Figure 6B-C). However, only 10% to 15% of those genes were up- or down-regulated in both subsets in the absence of ATG16L1 (Figure 6C & Online Table I). Ingenuity pathway analysis further highlighted the differential impact of autophagy in CD8α$^+$ versus CD11b$^+$ DCs. The top canonical pathways enriched in *Atg16l1* deficient versus WT CD11b$^+$ DCs (Figure 6D) corresponded to inositol (pyro)phosphate metabolism and phosphoinositide biosynthesis and degradation pathways, with major importance as cell signals in several biological processes, particularly relevant to the interface between cell signaling, membrane traffic and autophagy [27-29] as well as immune cell functions [30, 31]. The other major canonical pathways relate to atherosclerosis signaling and TGF-β signaling of high relevance to the immune response in atherosclerosis. Accordingly, the most enriched disease and biological functions categories corresponded to inflammatory response, cardiovascular disease (atherosclerosis and occlusion of artery) and metabolic

disease (diabetes mellitus), with a negative z-score indicating decreased bio-function in the absence of ATG16L1, and the most enriched physiological system development and function categories corresponded to lymphoid tissue structure and development, with a positive z-score for differentiation of Tregs, indicative of increased bio-function. None of these pathways was differentially expressed in *Atg16l1* deficient versus WT CD8α^+ DCs (Online Figure X). Further analysis revealed that *Atg16l1* deficient CD11b$^+$ DCs upregulated the expression of several genes implicated in immune tolerance and CD4$^+$ Treg expansion and function (Figure 6E) such as *Vdr*, *Aire*, *Foxj1*, *Sphk1*, *Havcr1* (also known as *Tim1*), *mir27*, *Tgfb3* and *Smad3*, most of which did not show significant differential expression in *Atg16l1* deficient versus WT CD8α^+ DCs (Online Table I). Thus, autophagy has a selective impact on CD11b$^+$ DCs with a major implication for their tolerogenic potential under HFD feeding in *Ldlr*$^{-/-}$ mice.

Splenic CD11b$^+$ DCs promote antigen specific CD4$^+$ Treg expansion in the presence of TGF-β.

In order to examine the ability of *Atg16l1* deficient and WT splenic CD11b$^+$ DCs to induce CD4$^+$ Tregs in vitro, we first used an antigen independent approach. Naïve (CD62L^{high}, CD44^{neg}, CD25^{neg}) CD4$^+$ T cells (from C57Bl/6J mice) were purified by flow cytometry (99% purity) and cultured with FACS-purified CD11b$^+$ DCs (99% purity) and soluble anti-CD3 ± TGF-β. In these conditions, we found no differences between WT and *Atg16l1* deficient DCs in the induction of CD4$^+$ Tregs (Online Figure XI). We then used antigen specific naïve OT-II CD4$^+$ T cells, which express a TCR specific to chicken ovalbumin (OVA), and cultured them with splenic CD8α^+ or CD11b$^+$ DCs in the presence of OVA protein ± TGF-β. First, we found that *Atg16l1* deficient CD8α^+ DCs were not able to induce T cell proliferation, as compared to WT CD8α^+ DCs (Online Figure XII A-B), in accordance with the role of autophagy in antigen presentation [17]. Interestingly however, *Atg16l1* deficiency did not alter antigen presentation in CD11b$^+$ DCs, which induced more T cell proliferation as compared to WT CD11b$^+$ DCs (Figure 7A). The addition of TGF-β reduced the number of cell divisions particularly in the presence of *Atg16l1* deficient CD11b$^+$ DCs, suggesting decreased T cell proliferation (Figure 7A-B). Interestingly, OVA-treated *Atg16l1* deficient CD11b$^+$ DCs seemed to enhance naïve OT-II cells production of IL-2, IFN-γ, and IL-6 in comparison with control DCs (Figure 7C). However, when TGF-β was added in the culture, OVA-treated *Atg16l1* deficient CD11b$^+$ DCs were no longer able to stimulate IFN-γ production by OT-II cells, promoted only a modest increase of IL-6, but were still able to induce a marked production of IL-2 in comparison with control DCs (Figure 7C). Co-culture of naïve OT-II cells with *Atg16l1* deficient CD11b$^+$ DCs in the absence of TGFβ seemed to prevent T cell polarization into CD4$^+$CD25$^+$Foxp3$^+$ Tregs (Figure 7D). However, the addition of TGFβ to the co-culture substantially increased the polarization of naïve OT-II cells into CD4$^+$CD25$^+$Foxp3$^+$ Treg cells in presence of *Atg16l1* deficient CD11b$^+$ DCs compared to WT CD11b$^+$ DCs (Figure 7E). This tolerogenic effect was restricted to *Atg16l1* deficient CD11b$^+$ DCs in the presence of TGFβ, and was not induced by incubation with *Atg16l1* deficient CD8α^+ DCs (Online Figure XII C-D). Finally, we examined the impact of *Atg16l1* deficiency on the uptake of oxLDL. While the latter was not affected by *Atg16l1* deficiency in macrophages, we found a slight reduction of oxLDL uptake by *Atg16l1* deficient compared to WT DCs (Online Figure XII E). However, the extent of oxLDL uptake was consistent between CD8α^+ and CD11b$^+$ DCs (Online Figure XII E).

Treatment with an anti-CD25 antibody prevents HFD-induced CD4$^+$ Treg expansion and abrogates the atheroprotective effect of autophagy deficiency in DCs.

In order to examine if the atheroprotective effect is dependent on CD4$^+$ Tregs, we generated *Atg16l1* cKO and control *Ldlr*$^{-/-}$ mice and treated them with a previously validated anti-CD25 antibody (ref) or an isotype control antibody during the 8 weeks of HFD feeding. Anti-CD25 treatment significantly reduced the percentages of Tregs, which were no longer different between *Atg16l1* cKO and control *Ldlr*$^{-/-}$ mice **(**Figure 8A) Systemic IL-2 levels were significantly increased in mice treated with anti-CD25, further supporting the efficiency of blocking the IL-2 receptor, and this was associated with a decrease of IL-10

(Figure 8B), a Treg related immunosuppressive and anti-atherogenic cytokine [32, 33]. We observed no differences in plasma lipid profiles or weight gain between the four groups of mice (Online Figure XIII). Analysis of atherosclerosis on aortic root cross sections showed that treatment with anti-CD25 completely abrogated the atheroprotective effect associated with *Atg16l1* deficiency in DCs (Figure 8C). The analysis of plaque phenotype revealed no significant differences in foam cell and SMC contents between the groups (Online Figure XIV A-B). However, treatment with anti-CD25 significantly increased T cell accumulation in *Atg16l1* cKO mice as compared to control *Ldlr*$^{-/-}$ mice (Online Figure XIV C). In addition, anti-CD25 treatment increased the acellular area in lesions of *Atg16l1 cKO* mice (Figure 8D), suggesting a more inflammatory and complex phenotype.

DISCUSSION

We show here that *Atg16l1* deletion in bone marrow-derived dendritic cells promotes Treg expansion and limits atherogenesis in *Ldlr*$^{-/-}$ mice fed a high fat diet. These effects are not due to *Atg16l1* deletion in CD8α^{+} DCs but to its deletion in the other CD11c-expressing cells. The latter include CD11b^{+} DCs, pDCs and some subsets of macrophages. However, ATG16L1 deletion in macrophages is unlikely to account for the athero-protective phenotype given the previously reported pro-atherogenic effect of abrogation of autophagy in macrophages [8, 9]. Importantly, our data indicate that CD11b^{+} DCs acquire tolerogenic properties after *Atg16l1* deletion, which promote Treg expansion, and reduce effector T cell accumulation and production of Th1-related cytokines in atherosclerotic lesions. Thus, in contrast to the pro-inflammatory and pro-atherogenic role of autophagy deficiency in macrophages [7-9], autophagy deficiency in DCs promotes a counter-regulatory immunosuppressive response that maintains vascular homeostasis in *Ldlr*$^{-/-}$ mice under HFD and limits the development of atherosclerosis.

Previous studies established a role for autophagy in antigen processing, loading on MHCII molecules and antigen presentation (reviewed in [17]). We found that this is the case with *Atg16l1* deficient CD8α^{+} DCs which were unable to (process and) induce antigen-specific proliferation of T cells in comparison to their WT CD8α^{+} DCs. Intriguingly however, the ability of CD11b^{+} DCs to induce antigen-specific T cell proliferation was not affected by *Atg16l1* deletion. In fact, we rather found increased antigen-specific T cell proliferation in presence of *Atg16l1* deficient compared to WT CD11b^{+} DCs. Interestingly, available data in the literature indicate that knockdown of *Atg16l1* in monocyte-derived DCs may induce more T cell proliferation in an alloreactive model [34], a finding attributed to increased DC numbers and expression of costimulatory molecules, and reduced expression of A20. However, *Atg16l1* deletion in our model did not affect DC numbers and none of those genes was significantly altered by *Atg16l1* deletion in DCs within the context of HFD-induced atherosclerosis. Thus, the reason for the differential impact of *Atg16l1* deletion on CD8α^{+} DC-dependent versus CD11b^{+} DC-dependent antigen-specific T cell proliferation remains unknown and merits further investigation.

Reduced T cell priming by *Atg16l1* deficient CD8α^{+} DCs in *Ldlr*$^{-/-}$ mice fed a HFD could have contributed to the observed decrease of aortic Th1 cells and the reduction of atherosclerosis, given the well validated pro-atherogenic role of Th1 immunity [24]. However, selective deletion of *Atg16l1* in CD8α^{+} DCs did not reproduce the phenotype. Moreover, the atheroprotection seen in *Ldlr*$^{-/-}$ mice with *Atg16l1* deficient DCs was dependent on Tregs, which were unaltered in *Ldlr*$^{-/-}$ mice with *Atg16l1* deficient CD8α^{+} DCs. This is consistent with the observation that CD8α^{+} DCs were unable to promote Treg expansion in vitro.

In contrast to CD8α^{+} DCs, *Atg16l1* deficiency in CD11b^{+} DCs substantially enhanced Treg generation in vitro, in the presence of TGF-β. This is a new finding, which could not be anticipated from previous observations. Xiong et al [35] reported increased Tregs in cardiac allograft recipient mice treated

with FLT3 and rapamycin compared to single treatments, and suggested a role for autophagy in Treg induction. However, DCs were not the only cells targeted by rapamycin in that experiment, and rapamycin could have exerted immune effects independent of its role in autophagy regulation. Chu et al reported reduced in vitro generation of $IL10^{+}Foxp3^{+}$ Tregs in the presence of *Atg16l1* deficient versus WT bone marrow monocyte-derived DCs when the cells were incubated with outer membrane vesicles (OMV) harvested from *B. fragilis* [36]. The total number of $Foxp3^{+}$ cells was not altered, and *Atg16l1* deficiency in DCs did not affect the generation of $IL10^{+}Foxp3^{+}$ Tregs in the absence of OMV. Moreover, the system does not involve antigen-specific presentation of OMV to T cells but the phenotype is attributed to alteration of DC inflammatory response by OMV. Thus, the data of Chu et al. apply to a very particular system and do not contradict nor invalidate our findings. In fact, our data initially suggested that, in the absence of TGF-β, the limited antigen-specific Treg induction that occurs in culture was rather reduced in the presence of *Atg16l1* deficient versus WT $CD11b^{+}$ DCs. This was not in line with our RNA-seq data, which showed significant differential upregulation of genes and pathways involved in the regulation of immune cell activation, the generation of Tregs and the induction of immune tolerance. A clue to this apparent discrepancy came from a closer look at the RNAseq data which revealed TGF-β signaling to be one of the most differentially upregulated pathways in *Atg16l1* deficient DCs in vivo. The high relevance of TGF-β is further attested by the importance of this cytokine in the in vivo generation and maintenance of Tregs, and the requirement for this cytokine to convert naïve $CD4^{+}CD25^{-}$ T cells into $Foxp3^{+}$ Tregs in vitro [37]. We therefore repeated the in vitro Treg generation experiment in presence of TGF-β and observed a substantial impact of *Atg16l1* deficiency in $CD11b^{+}$ DCs in boosting antigen-specific Treg generation compared to WT $CD11b^{+}$ DCs. Interestingly, this was associated with reduced production of IFN-γ, but increased production of IL-2, a cytokine that is essential for TGF-β-mediated conversion of naïve $CD4^{+}CD25^{-}$ T cells into $Foxp3^{+}$ Tregs and Treg expansion [38]. It remains unknown why Treg generation was not enhanced by *Atg16l1* deficient DCs when polyclonal $CD4^{+}$ T cells were used. However, the promotion of Treg expansion observed using the antigen-specific OT-II system nicely supports the in vivo RNAseq data and the impact of *Atg16l1* deficiency in DCs on Treg accumulation in $Ldlr^{-/-}$ mice fed a HFD. Whether additional mechanisms (e.g., modulation of cytokine production by DCs) contribute to the expansion of Tregs by autophagy-deficient DCs is currently unknown and will require further investigations.

A recent report found that Tregs ameliorate autoimmunity by restraining autophagy in DCs [39]. These findings are in line with our data and further support an important impact of autophagy on the tolerogenic potential of DCs. Interestingly, *Atg16l1* was the most significantly downregulated gene after interaction with Tregs, and this occurred through CTLA-4 dependent activation of the PI3K/Akt/mTOR axis, further highlighting, as in our RNAseq data, the close interconnection between inositol phosphate and 3-phosphoinositide pathways and the autophagy process, and their important consequences on DC biology and immune homeostasis.

Finally, we would like to mention that one of the most significantly downregulated gene in *Atg16l1* deficient versus WT DCs (whether $CD8\alpha^{+}$ or $CD11b^{+}$) was *Slc15a2*. This gene encodes a proton-coupled oligopeptide transporter recently found to mediate the transport of bacterially derived di-and tri-peptides that activate nucleotide-binding oligomerization domain (NOD) receptors in bone marrow-derived macrophages [40]. Although the relevance to atherosclerosis remains unknown, this finding may have important implications to the mechanisms of Crohn's disease. *NOD2* and *ATG16L1* genetic variants that lead to reduced function are associated with Crohn's disease. Reduced NOD2 activation has been shown to inhibit autophagy in DCs altering both bacterial trafficking and MHCII-dependent antigen presentation [41]. Our preliminary data may suggest that, in turn, reduced ATG16L1 function may inhibit bacterial dependent activation of NOD2 thereby altering the susceptibility to colitis. In this case, Treg maintenance in the absence of functional ATG16L1 may be acting as a safety break on intestinal inflammation. This hypothesis merits experimental testing.

In conclusion, we show that *Atg16l1* deficiency in murine CD11b^{+} DCs profoundly impact their phenotype towards a tolerogenic potential in *Ldlr*$^{-/-}$ mice fed a HFD, and reduces atherosclerosis through the expansion and maintenance of atheroprotective Tregs. Our results may have implications for immune-modulatory strategies to limit atherosclerosis through selective modulation of autophagy in DCs.

ACKNOWLEDGEMENTS
We thank Caetano Reis e Sousa, Francis Crick Institute, London, United Kingdom, for providing the *Clec9a*$^{+/cre}$ mice.

SOURCES OF FUNDING
This study was supported by the British Heart Foundation (CH/10/001/27642 and Grant No. 1659), and the European HEALTH 2013.1.3-3 programme.

DISCLOSURES
The authors declare no conflict of interest.

REFERENCES

1. Libby P, Lichtman AH, Hansson GK. Immune effector mechanisms implicated in atherosclerosis: from mice to humans. *Immunity*. 2013;38:1092-1104.
2. Ridker PM, Everett BM, Thuren T, et al. Antiinflammatory Therapy with Canakinumab for Atherosclerotic Disease. *N Engl J Med*. 2017;377:1119-1131.
3. Zhao TX, Mallat Z. Targeting the immune system in atherosclerosis. *J Am Coll Cardiol*. 2019; 73:1691-1706.
4. Grootaert MOJ, Moulis M, Roth L, Martinet W, Vindis C, Bennett MR, De Meyer GRY. Vascular smooth muscle cell death, autophagy and senescence in atherosclerosis. *Cardiovasc Res*. 2018;114:622-634.
5. Vion AC, Kheloufi M, Hammoutene A, et al. Autophagy is required for endothelial cell alignment and atheroprotection under physiological blood flow. *Proc Natl Acad Sci U S A*. 2017;114:E8675-E8684.
6. Grootaert MO, da Costa Martins PA, Bitsch N, Pintelon I, De Meyer GR, Martinet W, Schrijvers DM. Defective autophagy in vascular smooth muscle cells accelerates senescence and promotes neointima formation and atherogenesis. *Autophagy*. 2015;11:2014-2032.
7. Ouimet M, Franklin V, Mak E, Liao X, Tabas I, Marcel YL. Autophagy regulates cholesterol efflux from macrophage foam cells via lysosomal acid lipase. *Cell Metab*. 2011;13:655-667.
8. Razani B, Feng C, Coleman T, Emanuel R, Wen H, Hwang S, Ting JP, Virgin HW, Kastan MB, Semenkovich CF. Autophagy links inflammasomes to atherosclerotic progression. *Cell Metab*. 2012;15:534-544.
9. Liao X, Sluimer JC, Wang Y, Subramanian M, Brown K, Pattison JS, Robbins J, Martinez J, Tabas I. Macrophage autophagy plays a protective role in advanced atherosclerosis. *Cell Metab*. 2012;15:545-553.
10. Amersfoort J, Douna H, Schaftenaar FH, Foks AC, Kroner MJ, van Santbrink PJ, van Puijvelde GHM, Bot I, Kuiper J. Defective Autophagy in T Cells Impairs the Development of Diet-Induced Hepatic Steatosis and Atherosclerosis. *Front Immunol*. 2018;9:2937.
11. Hubbard VM, Valdor R, Patel B, Singh R, Cuervo AM, Macian F. Macroautophagy regulates energy metabolism during effector T cell activation. *J Immunol*. 2010;185:7349-7357.

12. Mocholi E, Dowling SD, Botbol Y, Gruber RC, Ray AK, Vastert S, Shafit-Zagardo B, Coffer PJ, Macian F. Autophagy Is a Tolerance-Avoidance Mechanism that Modulates TCR-Mediated Signaling and Cell Metabolism to Prevent Induction of T Cell Anergy. *Cell Rep*. 2018;24:1136-1150.
13. Xu X, Araki K, Li S, Han JH, Ye L, Tan WG, Konieczny BT, Bruinsma MW, Martinez J, Pearce EL, Green DR, Jones DP, Virgin HW, Ahmed R. Autophagy is essential for effector CD8(+) T cell survival and memory formation. *Nat Immunol*. 2014;15:1152-1161.
14. Wei J, Long L, Yang K, Guy C, Shrestha S, Chen Z, Wu C, Vogel P, Neale G, Green DR, Chi H. Autophagy enforces functional integrity of regulatory T cells by coupling environmental cues and metabolic homeostasis. *Nat Immunol*. 2016;17:277-285.
15. Ait-Oufella H, Sage AP, Mallat Z, Tedgui A. Adaptive (T and B cells) immunity and control by dendritic cells in atherosclerosis. *Circ Res*. 2014;114:1640-1660.
16. Cybulsky MI, Cheong C, Robbins CS. Macrophages and Dendritic Cells: Partners in Atherogenesis. *Circ Res*. 2016;118:637-652.
17. Ghislat G, Lawrence T. Autophagy in dendritic cells. *Cell Mol Immunol*. 2018;15:944-952.
18. Gil-Pulido J, Zernecke A. Antigen-presenting dendritic cells in atherosclerosis. *Eur J Pharmacol*. 2017;816:25-31.
19. Haddad Y, Lahoute C, Clement M, et al. The Dendritic Cell Receptor DNGR-1 Promotes the Development of Atherosclerosis in Mice. *Circ Res*. 2017;121:234-243.
20. Clement M, Haddad Y, Raffort J, Lareyre F, Newland SA, Master L, Harrison J, Ozsvar-Kozma M, Bruneval P, Binder CJ, Taleb S, Mallat Z. Deletion of IRF8 (Interferon Regulatory Factor 8)-Dependent Dendritic Cells Abrogates Proatherogenic Adaptive Immunity. *Circ Res*. 2018;122:813-820.
21. Mizushima N, Kuma A, Kobayashi Y, Yamamoto A, Matsubae M, Takao T, Natsume T, Ohsumi Y, Yoshimori T. Mouse Apg16L, a novel WD-repeat protein, targets to the autophagic isolation membrane with the Apg12-Apg5 conjugate. *J Cell Sci*. 2003;116:1679-1688.
22. Fujita N, Itoh T, Omori H, Fukuda M, Noda T, Yoshimori T. The Atg16L complex specifies the site of LC3 lipidation for membrane biogenesis in autophagy. *Mol Biol Cell*. 2008;19:2092-2100.
23. Mizushima N. Methods for monitoring autophagy using GFP-LC3 transgenic mice. *Methods Enzymol*. 2009;452:13-23.
24. Buono C, Binder CJ, Stavrakis G, Witztum JL, Glimcher LH, Lichtman AH. T-bet deficiency reduces atherosclerosis and alters plaque antigen-specific immune responses. *Proc Natl Acad Sci U S A*. 2005;102:1596-1601.
25. Ait-Oufella H, Salomon BL, Potteaux S, et al. Natural regulatory T cells control the development of atherosclerosis in mice. *Nat Med*. 2006;12:178-180.
26. Schraml BU, van Blijswijk J, Zelenay S, Whitney PG, Filby A, Acton SE, Rogers NC, Moncaut N, Carvajal JJ, Reis e Sousa C. Genetic tracing via DNGR-1 expression history defines dendritic cells as a hematopoietic lineage. *Cell*. 2013;154:843-858.
27. Lystad AH, Simonsen A. Phosphoinositide-binding proteins in autophagy. *FEBS Lett*. 2016;590:2454-2468.
28. Marat AL, Haucke V. Phosphatidylinositol 3-phosphates-at the interface between cell signalling and membrane traffic. *EMBO J*. 2016;35:561-579.
29. Itakura E, Kishi C, Inoue K, Mizushima N. Beclin 1 forms two distinct phosphatidylinositol 3-kinase complexes with mammalian Atg14 and UVRAG. *Mol Biol Cell*. 2008;19:5360-5372.
30. Okkenhaug K. Signaling by the phosphoinositide 3-kinase family in immune cells. *Annu Rev Immunol*. 2013;31:675-704.
31. Sauer K, Cooke MP. Regulation of immune cell development through soluble inositol-1,3,4,5-tetrakisphosphate. *Nat Rev Immunol*. 2010;10:257-271.
32. Mallat Z, Besnard S, Duriez M, Deleuze V, Emmanuel F, Bureau MF, Soubrier F, Esposito B, Duez H, Fievet C, Staels B, Duverger N, Scherman D, Tedgui A. Protective role of interleukin-10 in atherosclerosis. *Circ Res*. 1999;85:e17-24.

33. Mallat Z, Gojova A, Brun V, Esposito B, Fournier N, Cottrez F, Tedgui A, Groux H. Induction of a regulatory T cell type 1 response reduces the development of atherosclerosis in apolipoprotein E-knockout mice. *Circulation*. 2003;108:1232-1237.
34. Hubbard-Lucey VM, Shono Y, Maurer K, et al. Autophagy gene Atg16L1 prevents lethal T cell alloreactivity mediated by dendritic cells. *Immunity*. 2014;41:579-591.
35. Xiong A, Duan L, Chen J, Fan Z, Zheng F, Tan Z, Gong F, Fang M. Flt3L combined with rapamycin promotes cardiac allograft tolerance by inducing regulatory dendritic cells and allograft autophagy in mice. *PLoS One*. 2012;7:e46230.
36. Chu H, Khosravi A, Kusumawardhani IP, et al. Gene-microbiota interactions contribute to the pathogenesis of inflammatory bowel disease. *Science*. 2016;352:1116-1120.
37. Chen W, Jin W, Hardegen N, Lei KJ, Li L, Marinos N, McGrady G, Wahl SM. Conversion of peripheral CD4+CD25- naive T cells to CD4+CD25+ regulatory T cells by TGF-beta induction of transcription factor Foxp3. *J Exp Med*. 2003;198:1875-1886.
38. Zheng SG, Wang J, Wang P, Gray JD, Horwitz DA. IL-2 is essential for TGF-beta to convert naive CD4+CD25- cells to CD25+Foxp3+ regulatory T cells and for expansion of these cells. *J Immunol*. 2007;178:2018-2027.
39. Alissafi T, Banos A, Boon L, Sparwasser T, Ghigo A, Wing K, Vassilopoulos D, Boumpas D, Chavakis T, Cadwell K, Verginis P. Tregs restrain dendritic cell autophagy to ameliorate autoimmunity. *J Clin Invest*. 2017;127:2789-2804.
40. Hu Y, Song F, Jiang H, Nunez G, Smith DE. SLC15A2 and SLC15A4 Mediate the Transport of Bacterially Derived Di/Tripeptides To Enhance the Nucleotide-Binding Oligomerization Domain-Dependent Immune Response in Mouse Bone Marrow-Derived Macrophages. *J Immunol*. 2018;201:652-662.
41. Cooney R, Baker J, Brain O, Danis B, Pichulik T, Allan P, Ferguson DJ, Campbell BJ, Jewell D, Simmons A. NOD2 stimulation induces autophagy in dendritic cells influencing bacterial handling and antigen presentation. *Nat Med*. 2010;16:90-97.

FIGURE LEGENDS

Figure 1. Activation of the autophagic flux in dendritic cells under atherogenic conditions. A- Representative flow chart showing expression of LC3-GFP in $CD11c^{high}$ cells in the spleen of *Ldlr*$^{-/-}$ mice transplanted with LC3-GFP bone marrow and put under high fat diet (HFD) for 8 weeks. The inset represents the same staining from a wild type mouse (not expressing the LC3-GFP). **B-** Quantification of LC3-GFP MFI on $CD11b^+$ DCs in the spleen of *Ldlr*$^{-/-}$ mice transplanted with LC3-GFP bone marrow and left on chow diet (CD) or put under HFD for 8 weeks. *p= 0.0317 $CD11b^+$ DCs chow diet vs $CD11b^+$ DCs high fat diet, Mann-Whitney test. **C-** Representative histogram of flow cytometry showing the expression of LC3-GFP in $CD8\alpha^+$ and $CD11b^+$ DC under CD or HFD. FMO is the fluorescence minus one control. **D-** Flow charts depicting the gating strategy to analyze macrophages ($CD45^+CD11b^+F4/80^+$) and DCs ($CD45^+F4/80^-CD11c^+MHCII^{high}$) subsets ($CD11b^+$ DCs [$CD11b^+CD103^-$], double negative (DN) DCs [$CD11b^-CD103^-$], $CD103^+$ DCs [$CD11b^-CD103^+$]) as well as their expression of LC3-GFP, from the aorta of *Ldlr*$^{-/-}$ mice transplanted with LC3-GFP and kept under HFD for 8 weeks. A-D: n= 5 mice/group, **E-** Representative confocal images of DCs ($CD11c^+MHCII^+$, white arrows) and LC3 staining in atherosclerotic lesions from the aortic root of *Ldlr*$^{-/-}$ mice kept under HFD for 8 weeks. **F-** Representative flow histograms and quantification of the expression of LC3-GFP in splenic DC subsets ($CD8\alpha^+$ and $CD11b^+$ DCs) of *Ldlr*$^{-/-}$ mice transplanted with LC3-GFP bone marrow and put on HFD for 8 weeks. Chloroquine (CQ) was injected i.p. 48 and 24 hours before the end of the experiment to prevent the degradation of GFP by lysosomes. *p= 0.0379 $CD11b^+$ DCs high fat diet vs $CD11b^+$ DCs high fat diet + chloroquine, Mann-Whitney test. **G-** Representative flow histograms and quantification of the expression of LC3-GFP in aortic macrophages and DC subsets ($CD11b^+$, DN and $CD103^+$ DCs) of *Ldlr*$^{-/-}$ mice transplanted with LC3-GFP bone marrow and put on HFD for 8 weeks. Chloroquine (CQ) was administered as in F. F-G: n= 7 mice/group, *p= 0.0216 $CD103^+$ DCs high fat diet vs $CD103^+$ DCs high fat diet + chloroquine, Mann-Whitney test, data were obtained from one experiment.

Figure 2. *Atg16l1* deficiency in CD11c expressing cells promotes immune tolerance under HFD conditions in *Ldlr*$^{-/-}$ mice. A- Absolute number of immune cells in the spleen of Control (*Ldlr*$^{-/-}$ mice transplanted with *CD11c*$^{Cre-}$ *Atg16l1*$^{flox/flox}$ bone marrow) and *Atg16l1* cKO (*Ldlr*$^{-/-}$ mice transplanted with *CD11c*$^{Cre+}$ *Atg16l1*$^{flox/flox}$ bone marrow) mice after 8 weeks of HFD. n= 15 mice/group. **p= 0.0017 Control vs *Atg16l1* cKO, Mann-Whitney test. **B-** Absolute number of cDCs, $CD11b^+$ and $CD8\alpha^+$ DCs in the spleen of Control (n= 10) and *Atg16l1* cKO mice (n= 15) after 8 weeks of HFD, after flow cytometric analysis.
C- Representative flow chart showing the distribution of $CD8\alpha^+$ and $CD11b^+$ DC subsets in the spleen of Control and *Atg16l1* cKO mice after 8 weeks of HFD. **D-** Representative flow chart and quantification of MHC II expression by cDCs in the spleen of Control (n= 10) and *Atg16l1* cKO mice (n= 15) after 8 weeks of HFD. **p= 0.0014 Control DC vs *Atg16l1* cKO DC, Mann-Whitney test. **E-** Representative flow chart and quantification of CD80 expression by cDCs in the spleen of Control (n= 10) and *Atg16l1* cKO (n= 15) mice after 8 weeks of HFD. **F-** Absolute number of $CD4^+$ and $CD8^+$ T cells in the spleen of Control (n= 10) and *Atg16l1* cKO mice (n= 15) after 8 weeks of HFD, after flow cytometric analysis. ***p= 0.0006 number of splenic $CD4^+$ T cells and ***p< 0.0001 number of splenic $CD8^+$ T cells in control vs *Atg16l1* cKO mice, Mann-Whitney test. **G-** Representative flow chart of CD44 expression by $CD4^+$ T cells and quantification of the percentage of $CD4^+$ and $CD8^+$ T cells expressing CD44 in the spleen of Control (n= 10) and *Atg16l1* cKO mice (n= 15) after 8 weeks of HFD. **H-** Quantification and representative flow charts showing the proportion of $CD4^+$ Tregs ($Foxp3^+CD25^{high}$) in the spleen of Control (n= 10) and *Atg16l1* cKO mice (n= 15) after 8 weeks of HFD. *p= 0.0137, %$CD4^+$ Tregs in control vs *Atg16l1* cKO mice, Mann-Whitney test.
A-H: Results are representative of 3 independent experiments.

Figure 3. *Atg16l1* deficiency in CD11c expressing cells promotes a shift of the effector/regulatory T cell balance in the aorta towards an anti-atherogenic phenotype in *Ldlr*$^{-/-}$ mice.

A- Representative flow charts and quantification of DC subsets in the aorta of Control and *Atg16l1* cKO mice after 8 weeks of HFD (n= 9 mice/group). **B, C**- Representative flow charts and quantification of IFN expressing T cells (B) and $CD4^+$ Tregs (C) in the aortas of Control and *Atg16l1* cKO mice after 8 weeks of HFD (n= 9 mice/group). B- *p= 0.0441 $\%CD4^+$ $IFN\gamma^+$ within aortic $CD45^+$ cells from control vs *Atg16l1* cKO mice, Mann-Whitney test. C- *p= 0.0454, $\%CD4^+$ $Foxp3^+$ within aortic $CD45^+$ cells from control vs *Atg16l1* cKO mice, Mann-Whitney test. Graphs represent data pooled from 2 independent experiments.
D, E- Representative pictures of Oil red O staining and quantification of atherosclerotic lesions in the aortic sinus (D) and in the "en face" thoracic aorta (E) of Control (n=15 mice) and *Atg16l1* cKO (n=15 mice) mice after 8 weeks of HFD. D- p= 0.0002 between genotypes, 2 way-ANOVA followed by uncorrected Fisher's test; *p= 0.0356 **p= 0.0098 Control vs *Atg16l1* cKO mice at indicated levels. E- *p= 0.0411 Control vs *Atg16l1* cKO mice, Mann-Whitney test. **F**- Representative pictures of Hoechst staining and quantification of acellular area in the atherosclerotic lesions of Control and *Atg16l1* cKO mice after 8 weeks of HFD (n=15 mice/group). *p= 0.0454, Control vs *Atg16l1* cKO mice, Mann-Whitney test.
D-F: Data are pooled from 2 independent experiments.

Figure 4. T cell depletion abrogates the athero-protective effect of *Atg16l1* deficiency in CD11c expressing cells. A- Quantification and representative flow charts of $CD4^+$ and $CD8^+$ T cells in the spleen of Control and *Atg16l1* cKO mice after 8 weeks of HFD and treatment with anti-CD4/CD8 (150 µg/mouse, i.p., weekly). Inset shows a representative staining of CD4 and CD8 in a non-depleted mouse. **B, C**- Representative pictures of Oil red O staining and quantification of atherosclerotic lesions in the "en face" thoracic aorta (B) and in the aortic sinus (C) of Control and *Atg16l1* cKO mice after 8 weeks of HFD and T cell depletion. **C**- p= 0.0011 between genotypes, 2-way ANOVA followed by an uncorrected Fisher's test: **p= 0.008 level 600 µm, **p= 0.0076 level 800 µm, Control vs *Atg16l1* cKO treated with anti-CD4/CD8. **D-F**- Quantification and representative pictures of the density (% of positive staining area to total lesion area) of MOMA-2 staining (D, foam cells, *p=0.0408, Mann-Whitney test, control vs *Atg16l1* cKO mice), αSMA staining (SMCs, E) and acellular area (F, *p=0.0111, Mann-Whitney test, control vs *Atg16l1* cKO mice), by immunofluorescent microscopy, on aortic sinus cross sections from Control and *Atg16l1* cKO mice after 8 weeks of HFD and T cell depletion. In D and E, small pointed line depicts the atherosclerotic lesion. In F, dashed line depicts the acellular area.
A-F: n= 7 mice/group. Data were obtained from one experiment.

Figure 5. *Atg16l1* deficiency in $CD8\alpha^+$ DCs does not induce immune tolerance and does not protect against atherosclerosis in *Ldlr*$^{-/-}$ mice. A- Strategy for conventional DC (cDC) purification from the spleen of $CD11c^{Cre+}$ $Atg16^{flox/flox}$, $Clec9a^{Cre+}$ $Atg16l1^{flox/flox}$ and control mice ($CD11c^{Cre-}$ $Atg16^{flox/flox}$ and $Clec9a^{Cre-}$ $Atg16^{flox/flox}$) and analysis of *Atg16l1* expression by RT-QPCR (normalized on 36B4). n= 5-6 mice/group; p<0.0001 for comparisons between all groups (Kruska-Wallis); post-hoc uncorrected Dunn's test, ***p= 0.0003 DC $CD8\alpha^+$ $CD11c^{Cre+}$ $Atg16^{flox/flox}$; ***p= 0.0008 DC $CD8\alpha^+$ $Clec9a^{Cre+}$ $Atg16^{flox/flox}$ vs DC $CD8\alpha^+$ control; *p= 0.056 DC $CD11b^+$ $CD11c^{Cre+}$ $Atg16^{flox/flox}$ vs DC $CD11b^+$ control. **B**- Representative flow chart showing the distribution of $CD8\alpha^+$ and $CD11b^+$ DC subsets and the quantification of the proportion of cDCs in the spleens of $Clec9a^{Cre+}$ $Atg16^{flox/flox}$ and Control mice after bone marrow transplantation (BMT) in *Ldlr*$^{-/-}$ mice and 8 weeks of HFD. **C**- Representative flow chart showing the distribution of $CD8^+$ and $CD4^+$ T cells and the quantification of the proportion of each subset in the spleens of $Clec9a^{Cre+}$ $Atg16^{flox/flox}$ and Control mice after BMT in *Ldlr*$^{-/-}$ mice and 8 weeks of HFD. **D**- Representative flow chart showing the proportion of IFNγ producing $CD4^+$ T cells, and the quantification, in the spleens of $Clec9a^{Cre+}$ $Atg16^{flox/flox}$ and Control mice after BMT in *Ldlr*$^{-/-}$ mice and 8 weeks of HFD**. E**- Representative flow chart showing the proportion of $CD4^+$ Tregs ($CD3^+CD4^+Foxp3^+CD25^{high}$), and the quantification in the spleens of $Clec9a^{Cre+}$ $Atg16^{flox/flox}$ and Control mice after BMT in *Ldlr*$^{-/-}$ mice and 8 weeks of HFD. **F, G**- Quantification and representative pictures of Oil red O staining for atherosclerotic lesions analysis on "en face" thoracic aorta (F) and in the aortic sinus (G) of $Clec9a^{Cre+}$ $Atg16^{flox/flox}$ and Control mice after BMT in *Ldlr*$^{-/-}$ mice and 8

weeks of HFD. B-E, G: 7-8 mice/group. F: 6 mice/group. Data are representative of 2 independent experiments.

Figure 6. ***Atg16l1*** **deficiency in CD11b$^+$ DCs under atherogenic conditions promotes a tolerogenic gene expression program. A**- Experimental strategy for the purification of DCs before RNA-seq. DCs were purified from 3 Control mice and 2 *Atg16l1* cKO mice. **B**- Venn diagram showing the proportion of differentially expressed genes between CD11b$^+$ and CD8α^+ DC, normalized on the level of expression from control DCs (FDR<0.1, p<0.002). **C**- Volcano plot showing the level of expression of the differentially expressed genes from CD11b$^+$ DCs *Atg16l1* cKO compared to wild-type CD11b$^+$ DCs (FDR<0.1, p<0.002). **D**- Ingenuity analysis of the top 10 canonical pathways in CD11b$^+$ DCs of *Atg16l1* cKO mice.
E- Ingenuity analysis of the top disease and bio-functions categories in CD11b$^+$ DCs of *Atg16l1* cKO mice.
F- Ingenuity analysis of the top physiological system development categories in CD11b$^+$ DCs of *Atg16l1* cKO mice.

Figure 7. ***Atg16l1*** **deficiency in CD11b$^+$ DCs promotes polarization of antigen specific CD4$^+$ Treg under TGFβ supplementation in vitro. A, B**- Representative flow chart and quantification of naïve OTII cell proliferation (using cell trace violet, generations are shown in A) after co-culture with OVA protein and FACS-purified (control and *Atg16l1* cKO) CD11b$^+$ DC in the absence (**A**) or presence of TGFβ (**B**). Data were obtained using technical replicates and are representative of 2 independent experiments. **C** and **D-** Cytokine quantification by multiplex CBA beads of IL2, IFNγ, TNF, IL6 and IL17 in the supernatants of naïve CD4+ OT-II T cells co-cultured for 5 days with CD11b$^+$ DCs from control or *Atg16l1* cKO mice in the presence of OVA ± TGFβ. Data were obtained using technical replicates and are representative of 2 independent experiments. **E** and **F**- Representative flow chart and quantification of the proportion of CD4$^+$ Tregs (Foxp3$^+$CD25^{high}) generated from naïve OTII CD4$^+$ T cells after 5 days of co-culture with control or *Atg16l1* cKO CD11b$^+$ DC with OVA only (E) or OVA + TGFβ (F). Data were obtained using technical replicates and are representative of 2 independent experiments.

Figure 8. Treatment with anti-CD25 (PC61) antibody abrogates the athero-protective effect of ***Atg16l1*** **deficiency in CD11c expressing cells. A**- Representative flow chart and quantification of Foxp3 expressing CD4$^+$ T cells in the spleens of *Atg16l1* cKO and Control mice treated with isotype-matched or anti-CD25 antibody, starting at the beginning of the HFD (250µg of antibody/mouse/week, for 8 weeks). **p= 0.0066, Control + isotype vs *Atg16l1* cKO + isotype Mann-Whitney test; p=0.1393, Control + anti-CD25 vs *Atg16l1* cKO + anti-CD25, Mann-Whitney test**. B**- IL-2 and IL-10 titration in the plasma of Control and *Atg16l1* cKO mice infused with isotype-matched or anti-CD25 antibody. Control + isotype, n= 19; *Atg16l1 cKO* + isotype, n= 18; Control + anti-CD25, n= 8; *Atg16l1 cKO* + anti-CD25, n= 8. **C**- Representative pictures and quantification of atherosclerotic lesions using Oil red O staining at the level of the aortic sinus from *Atg16l1* cKO and Control mice after BMT in *Ldlr*$^{-/-}$ mice and 8 weeks of HFD, and treatment with isotype-matched or anti-CD25 antibody. 2-way ANOVA followed by an uncorrected Fisher's test: *p= 0.0376 level 200 µm, p= 0.0498 level 400 µm, Control vs *Atg16l1* cKO treated with isotype; Control vs *Atg16l1* cKO treated with anti-CD25, 2-way ANOVA p=0.3544. Control + isotype, n= 10; *Atg16l1 cKO* + isotype, n= 8; Control + anti-CD25, n= 8; *Atg16l1 cKO* + anti-CD25, n= 8. **D**- Representative pictures and quantification of acellular area in atherosclerotic lesions of *Atg16l1* cKO and Control mice after BMT in *Ldlr*$^{-/-}$ mice and 8 weeks of HFD, and treatment with isotype-matched or anti-CD25 antibody. **p= 0.0041 control vs *Atg16l1* cKO mice treated with isotype, Mann-Whitney test; **p= 0.003 control vs *Atg16l1* cKO mice treated with anti-CD25, Mann-Whitney test.

NOVELTY AND SIGNIFICANCE

What Is Known?

- Autophagy in macrophages limits atherosclerosis.
- Dendritic cells (DCs) modulate the development of atherosclerosis. However, the role of autophagy in DC function during atherosclerosis is unknown.

What New Information Does This Article Contribute?

- *Atg16l1* deficiency in DCs prevents experimental atherosclerosis in a regulatory T (Treg) cell dependent manner.
- TGFβ signaling is enhanced in splenic *Atg16l1* deficient $CD11b^+$ DCs under high fat and high cholesterol feeding.
- *Atg16l1* deficient DCs promote the differentiation of antigen specific $CD4^+$ Tregs in the presence of TGFβ.

Dendritic cells are professional antigen presenting cells able to prime naive $CD4^+$ T cells and drive their polarization toward a pro-inflammatory or tolerogenic phenotype. Pro-inflammatory IFNγ-producing $CD4^+$ T cells promote atherosclerosis whereas $CD4^+$ Tregs prevent it. Better understanding of the mechanisms involved in the polarization of naïve $CD4^+$ T cells in experimental atherosclerosis will help to identify new therapeutic strategies. Here, we addressed the role played by autophagy in DCs during $CD4^+$ T cell priming/polarization in atherosclerosis. Autophagy disruption in DCs halted the development of atherosclerosis in *Ldlr*$^{-/-}$ mice fed a high fat/high cholesterol diet and was associated with a preferential expansion of $CD4^+$ Tregs. T cell depletion and specific $CD4^+$ Treg depletion prevented this atheroprotective effect. Ex-vivo RNA-seq analysis revealed a TGFβ signaling signature in autophagy deficient splenic $CD11b^+$ DCs. In vitro experiments revealed that autophagy deficient $CD11b^+$ DCs promoted the polarization/expansion of antigen specific $CD4^+$ Tregs from naïve $CD4^+$ Tcells. Taken together, our data show that the manipulation of autophagy in $CD11b^+$ DCs may be an interesting strategy to interfere with the development of atherosclerosis.

FIGURE 1

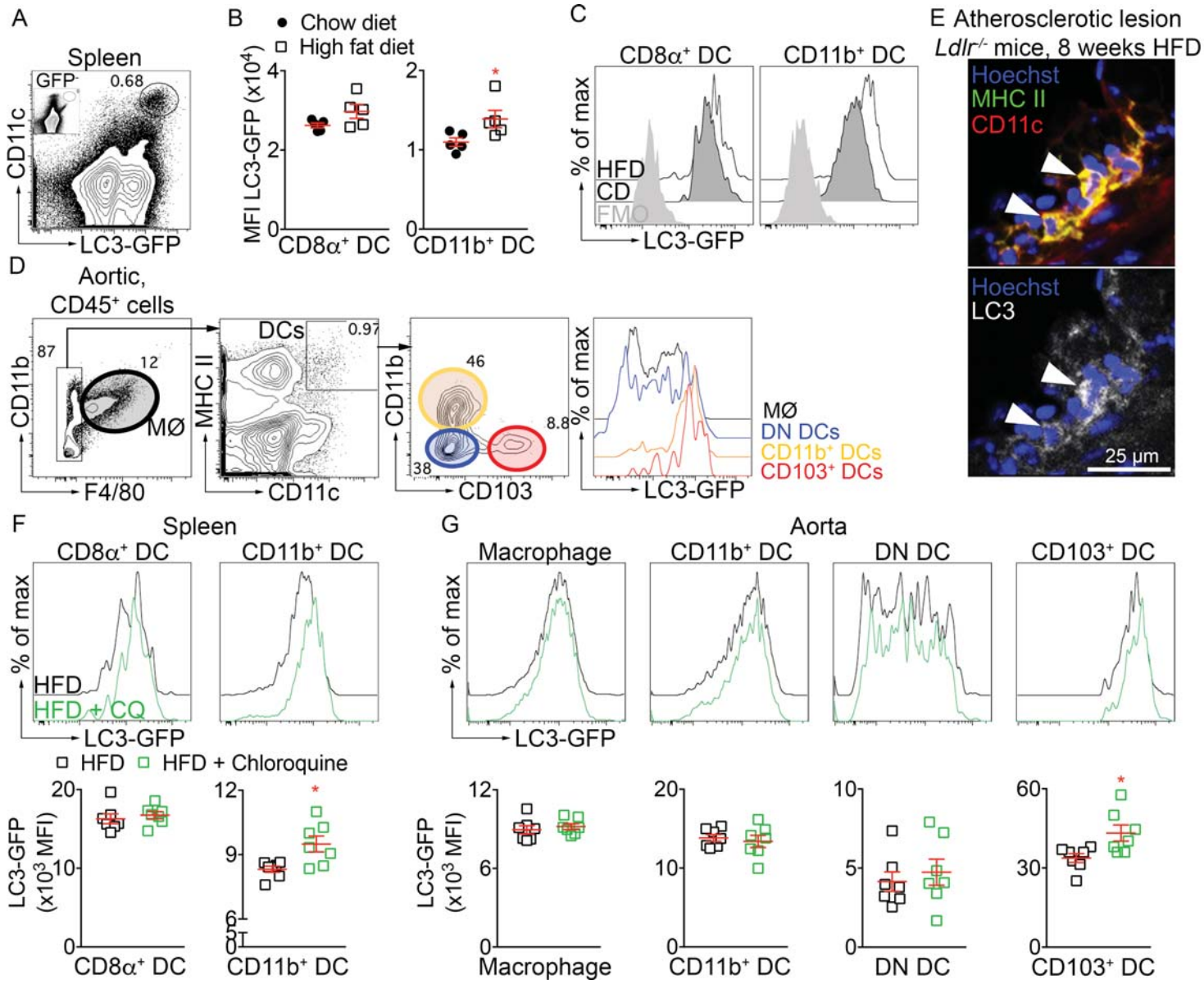

FIGURE 2

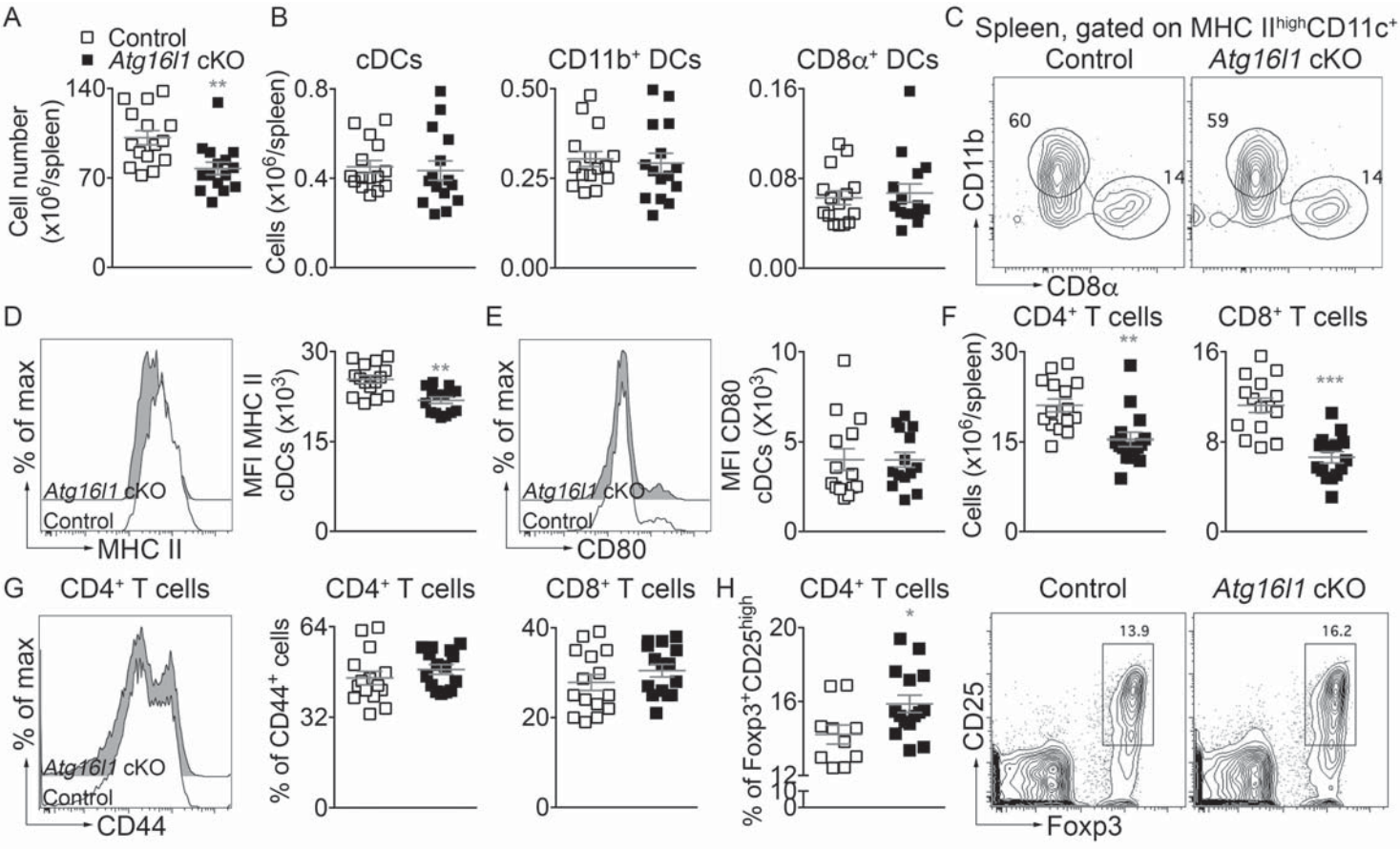

FIGURE 3

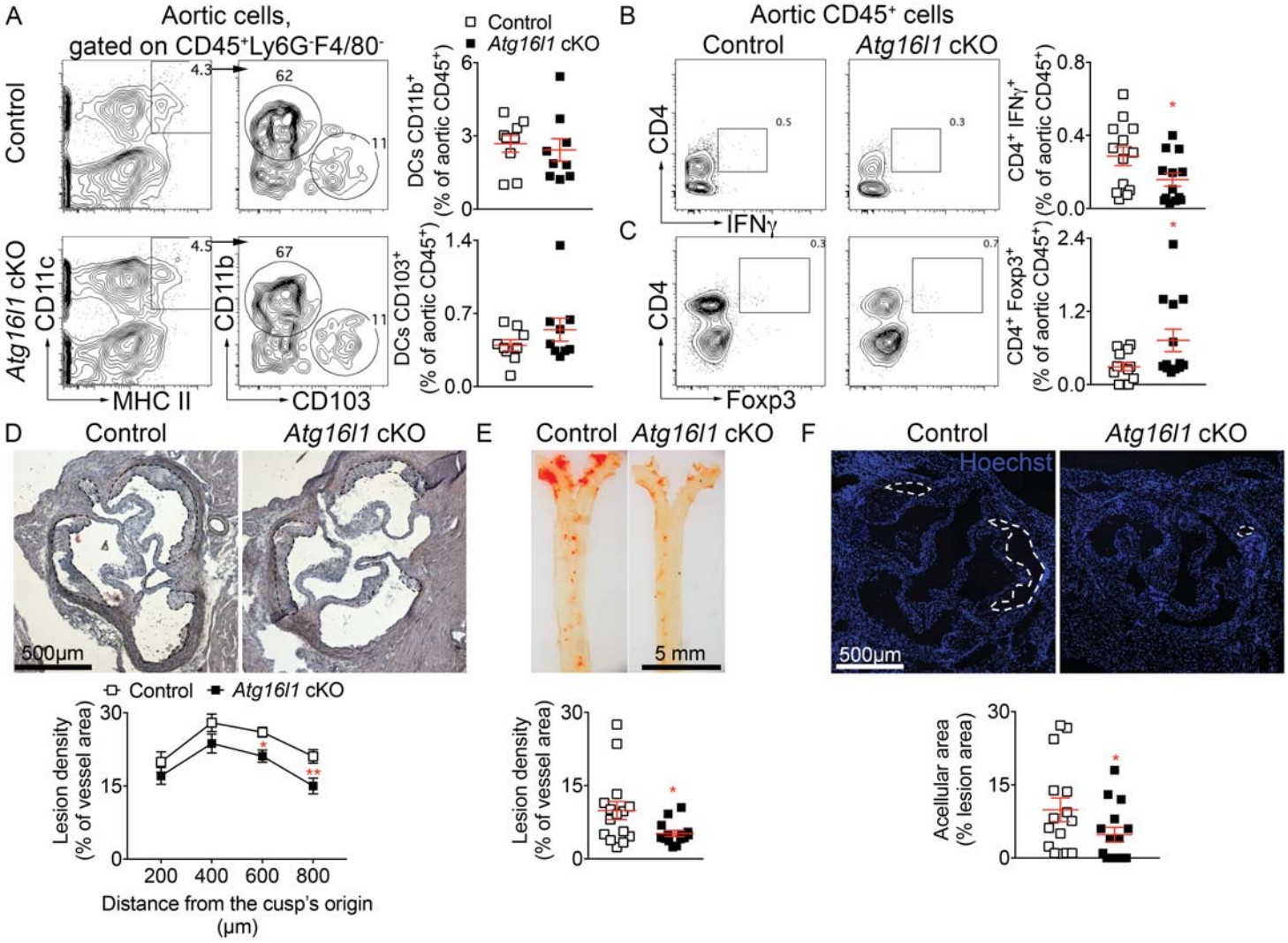

FIGURE 4

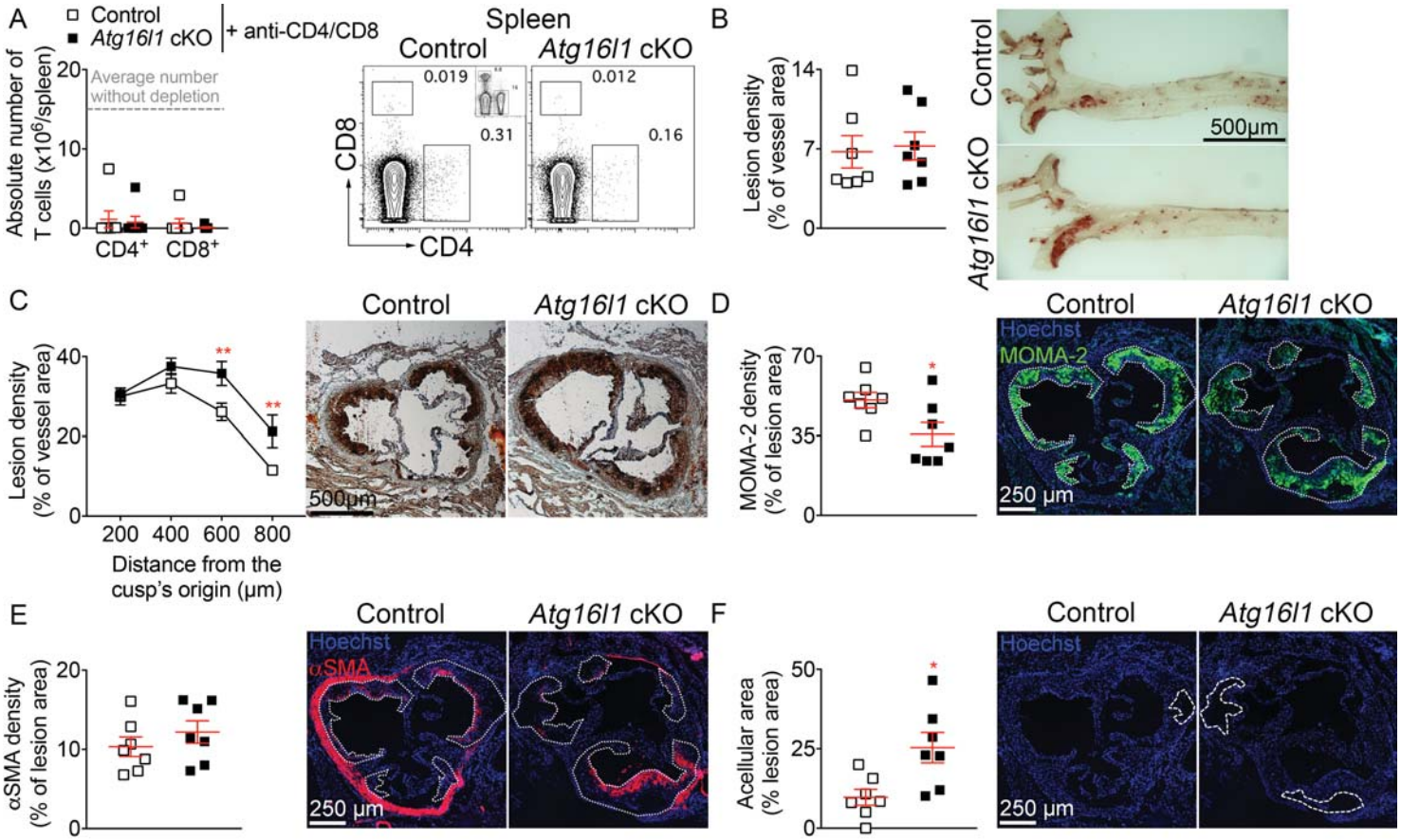

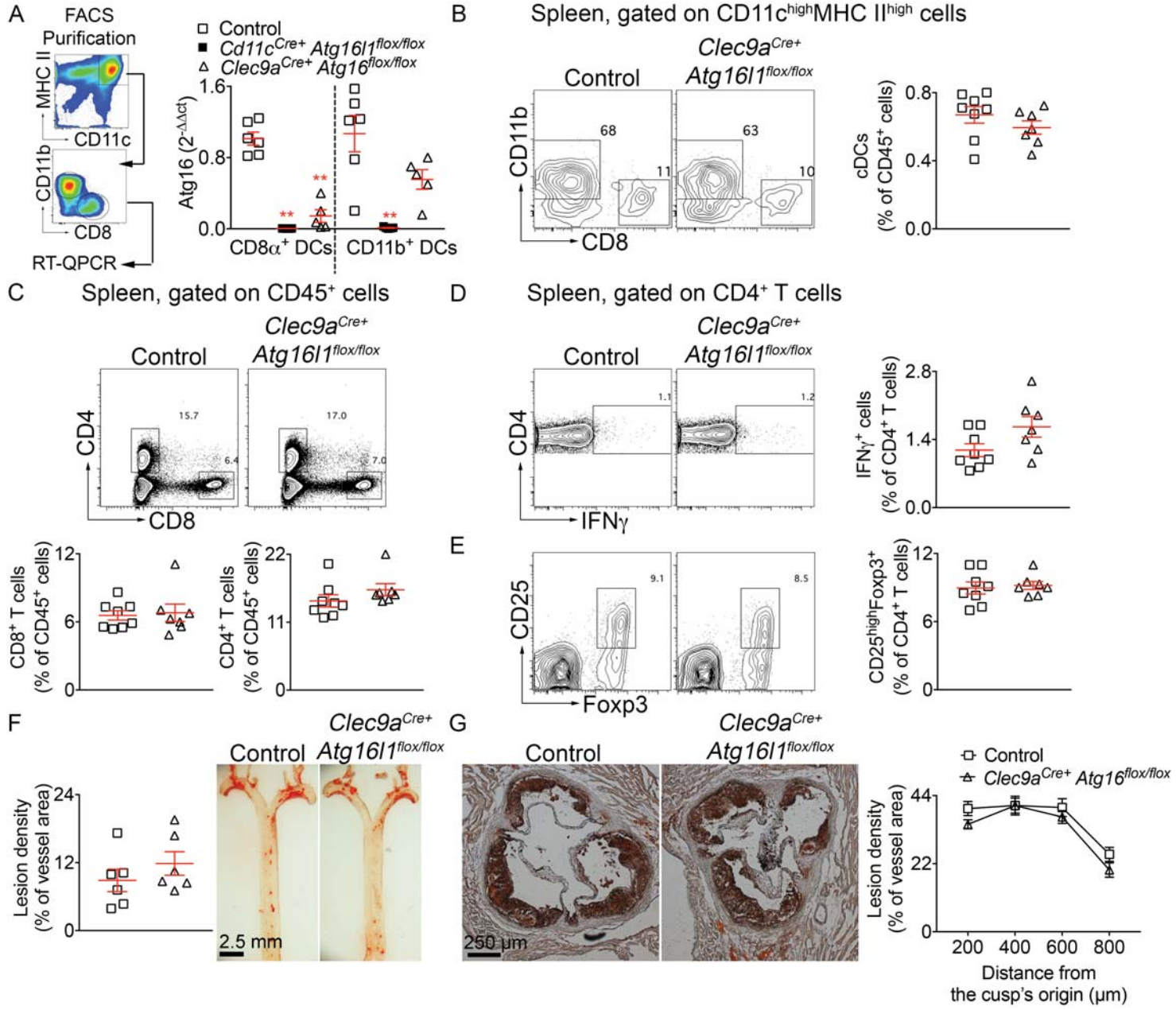

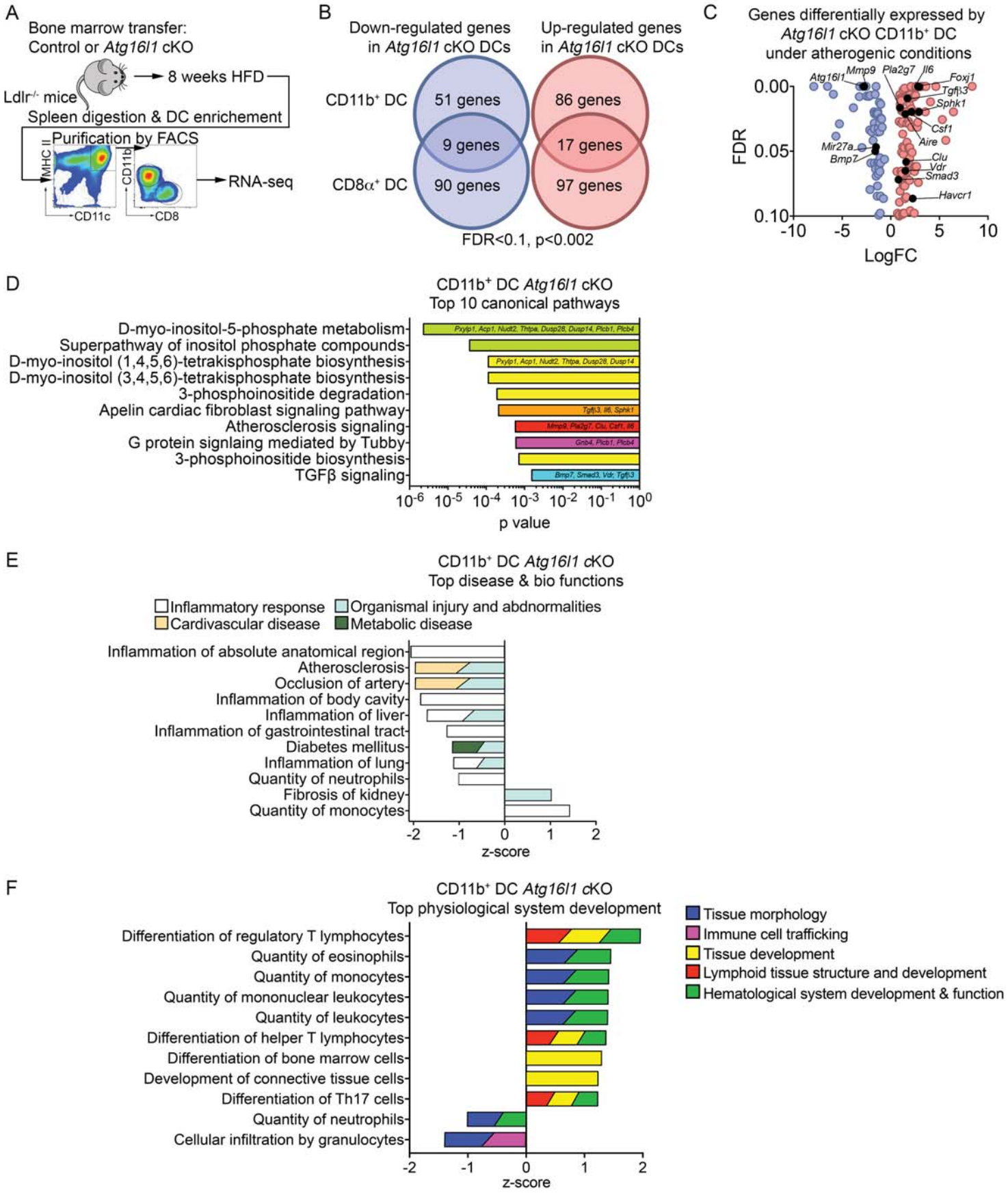

FIGURE 7